Low Temperature Physics/Fizika Nizkikh Temperatur, 2017, v. 43, No. 8, pp. 1224–1228

Synthesis, crystal structure, electric and magnetic properties of new $UNiSi_2$ splat

Z. Molčanová[1], M. Mihalik[1], M. Mihalik, Jr.[1], M. Rajňák[1], M. Zentková[1], M. Huráková[1], V. Kavečanský[1], M. Paukov[2], L. Havela[2], M. Cieslar[2], and K. Milianchuk[2,3]

[1]*Institute of Experimental Physics SAS, Watsonova 47, 040 01 Košice, Slovakia*

[2]*Charles University, Faculty of Mathematics and Physics, Ke Karlovu 5, 121 16 Prague 2, Czech Republic*

[3]*Ivan Franko National University of Lviv, 1 Universytetska Str., Lviv 79000, Ukraine*

E-mail: zentkova@saske.sk

Received January 31, 2017, published online June 26, 2017

We explored the crystal structure, magnetic and transport properties of $UNiSi_2$ material, which was prepared by rapid solidification — splat cooling. The $UNiSi_2$ splat is mostly single phase, the refinement of crystal structure indicated orthorhombic $CeNiSi_2$-type structure (space group *Cmcm*) with lattice parameters a = 4.0082 Å, b = 16.0813 Å and c = 4.0064 Å. Also SEM analysis revealed the morphology exhibiting dendritic grains in the matrix. TEM images indicate mixed structure formed by crystalline particles embedded into amorphous or nanocrystalline matrix. Magnetic and electrical properties of the splat resemble properties of samples, which were prepared by conventional methods, exhibiting a ferromagnetic transition at about 91 K and similar temperature dependence of resistivity. The coercive field of $\mu_0 H_c$ = 2.25 T is much enhanced due to the magnetic anisotropy introduced by the sample preparation technique. Barkhausen jumps were observed on the hysteresis loop. Magnetization of the sample does not saturate in magnetic fields up to $\mu_0 H$ = 18 T.

PACS: **75.50.–y** Studies of specific magnetic materials;
75.50.Tt Fine-particle system; nanocrystalline materials.

Keywords: magnetic anisotropy, Barkhausen jumps, magnetic hysteresis, $UNiSi_2$ splat.

1. Introduction

Research of strongly correlated electron systems is very attractive part of the physics of condensed matter. Materials with strongly correlated electrons, originating in open *d*- or *f*-shells, have often unusual electrical and magnetic properties [1,2]. In the case of actinides there are mainly uranium-based intermetallic compounds, exhibiting diverse exotic types of effects, as unconventional type of magnetism or superconductivity [3], often accompanying by heavy fermion behavior [4–7]. On the other hand, the study of uranium compounds is stimulated by the practical use of nuclear energy (nuclear fuel or waste) [8–10].

The splat cooling technique can facilitate stabilization of selected polymorphous modifications. It was successfully used for retention of high-temperature γ-uranium phase to room temperature [11]. It can be expected that the rapid solidification can stimulate preparation of single phase from in-congruently melting materials, e.g., $UNiSi_2$.

The uranium compound $UNiSi_2$ melts incongruently, however single crystals of this compound were grown by the Czochralski method [12] and in a gallium flux [13]. This compound crystallizes in the orthorhombic $CeNiSi_2$-type layered structure (space group *Cmcm*) [14], which is constructed from deformed fragments of the $CeGa_2Al_2$ and α-$ThSi_2$ structures. $UNiSi_2$ exhibits ferromagnetism with local uranium moments below the Curie temperature T_C = = 95 K [15–17], while a Kondo lattice behavior was reported at higher temperatures [13,15,16]. The residual resistance can be enhanced by high pressure of about 5.5 GPa [13]. A strong magnetic anisotropy was observed on the single crystal with the easy magnetization direction in the *ac* plane [12]. The electronic coefficient γ is small in comparison with uranium heavy fermion compounds [16]. In the present paper we report on synthesis, characterization, electrical and magnetic properties of samples with nominal compositions $UNiSi_2$, which were prepared by the splat cooling technique and we compare our results with previous re-

sults, which were obtained on polycrystalline materials and single crystals [12–17].

2. Experimental results

In the first step, polycrystalline sample of $UNiSi_2$ was prepared by arc melting from the starting constituents in Ar atmosphere. For better homogeneity, the sample was several times turned over and re-melted. The obtained ingot was subsequently placed into the high vacuum splat cooling system. In this technique, an alloy is melted by electrical arc under Ar atmosphere. The molten drop then falls through a hole in a copper crucible, triggering an infrared photoelectric switch that initiates movement of two massive copper anvils, which hit the drop producing a splat, which is a foil of irregular shape and typical thickness 0.1 mm. X-ray powder diffraction (XRPD) measurements were performed by Rigaku Ultima IV diffractometer in Bragg Brentano configuration and as a source we used $Cu_{K\alpha1,\alpha2}$ doublet radiation ($\lambda_{K\alpha1}$ = 0.154060 nm, $\lambda_{K\alpha2}$ = 0.1544430 nm). Additional analysis was performed by TESCAN VEGA3 scanning electron microscope (SEM) using secondary electrons and back scattered electrons imaging as well energy dispersive x-ray (EDX) analysis and transmission electron microscopy (TEM) using a JEOL JEM 2000 FX microscope equipped with a thin-window x-ray energy dispersive analyser (EDX).

The magnetic measurements were carried out by the SQUID magnetometer in MPMS and in applied magnetic field up to 5 T in the temperature range 2–300 K. High magnetic field experiments were performed on the Cryogen Free High Field Measurement System (Cryogenic Ltd.) operating in magnetic field up to 18 T. The electrical resistivity was measured by ac transport method in the temperature range 5–380 K by the PPMS.

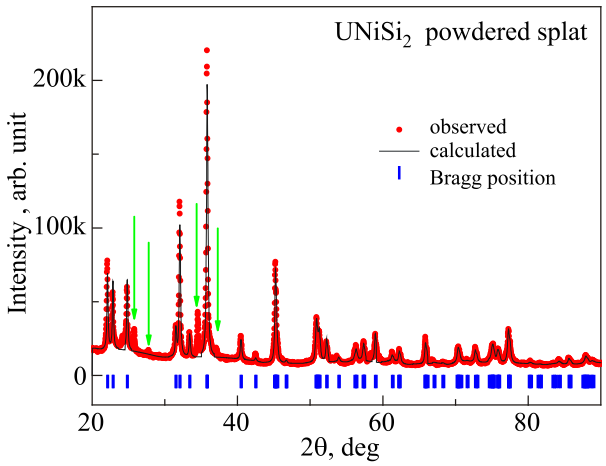

Fig. 1. (Color online) X-ray diffraction pattern of the $UNiSi_2$ splat are shown together with Bragg's position for main phase $UNiSi_2$. The secondary phase is indicated by arrows.

3. Results and discussion

XRPD measurements from both the surface of splat and the powdered splat revealed that $UNiSi_2$ contains only small traces of spurious phases. The XRPD patterns were fitted using Le Baill method and using orthorhombic, $CeNiSi_2$-type structure as a starting model [14].

The refined lattice parameters are a = 4.0082 Å, b = = 16.0813 Å and c = 4.0064 Å. We have also detected the presence of a secondary phase (Fig. 1), however we were unable to determine the chemical composition of this phase due to very low contribution from this phase to the total XRPD pattern.

The SEM analysis from the surface of the polished $UNiSi_2$ rapidly cooled samples (splats) indicates that the average composition corresponds to the nominal one. Also

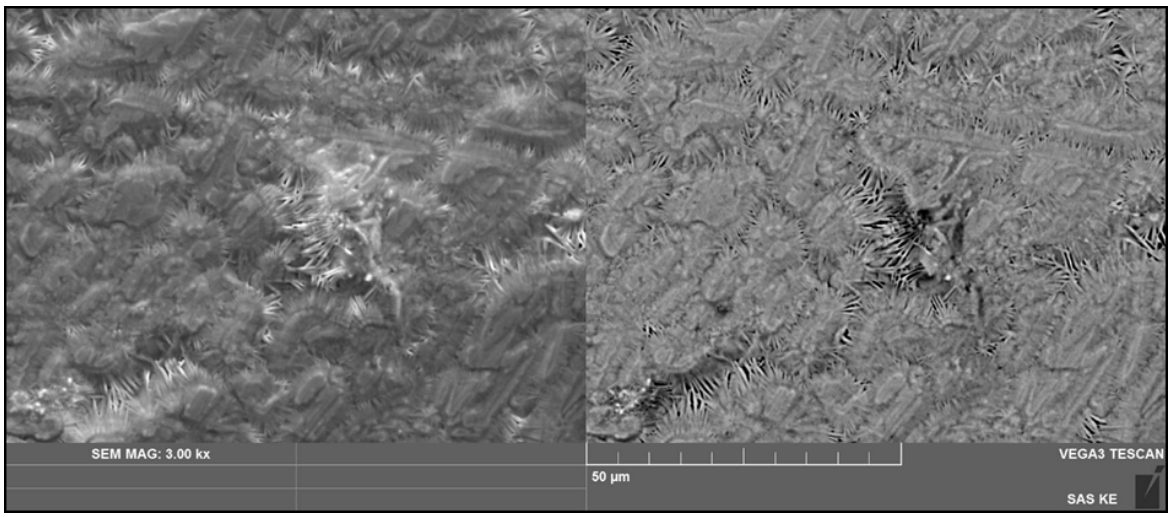

Fig. 2. SEM image was taken from the surface in secondary (left) and backscattered (right) electrons.

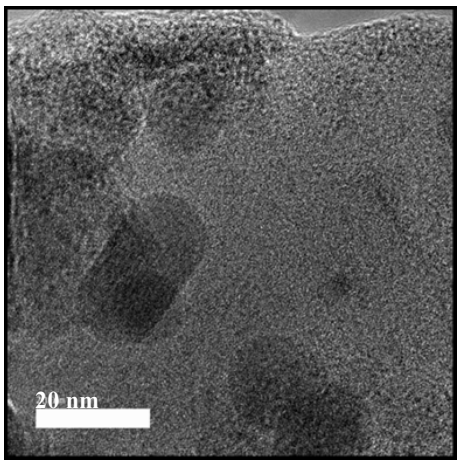

Fig. 3. TEM image of the $UNiSi_2$ splat shows mixture structure consisting of well-defined crystals embedded into the amorphous or very fine nanocrystalline matrix.

the morphology exhibits dendritic grains, which are nickel-depleted due to quenching (Fig. 2). The TEM revealed mixed structure formed cylindrical or spherical nanocrystalline particles which are embedded into amorphous or nanocrystalline matrix with very fine nanoparticles (Fig. 3). The cylindrical particles have average size of about 20×10 nm. The remaining part of splat contains large crystalline blocks with the partially distorted crystal structure.

The results of ac susceptibility measurements suggest that the $UNiSi_2$ polycrystalline sample has magnetic transition at 91 K (Fig. 4) as it is evident from pronounced broad

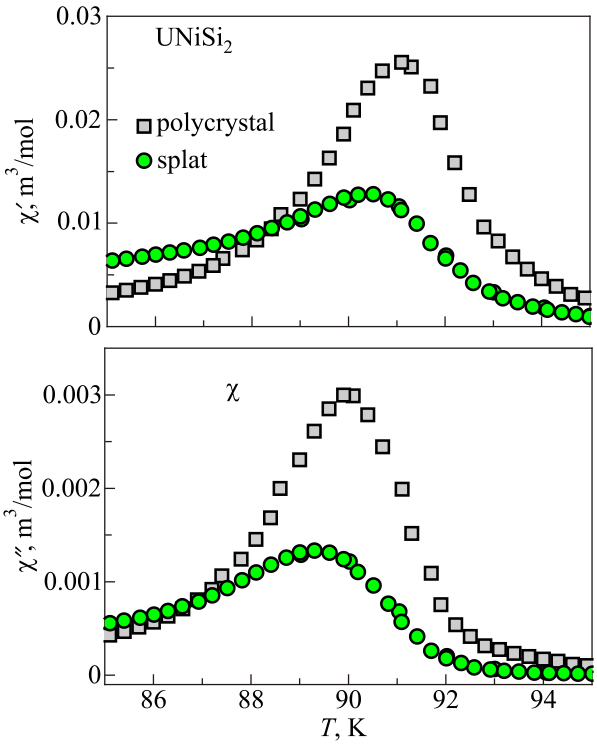

Fig. 4. (Color online) ac susceptibility for polycrystalline is compared with ac susceptibility of splat.

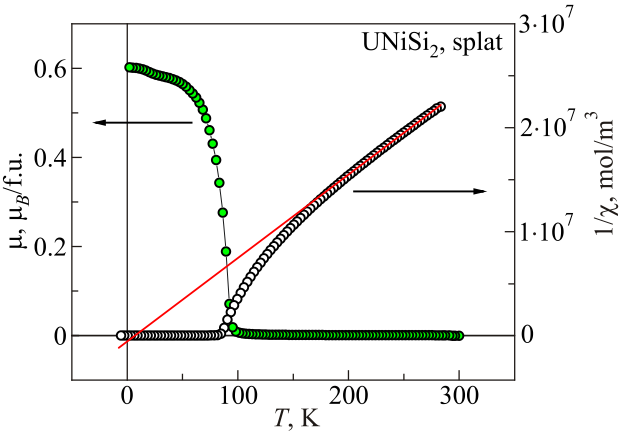

Fig. 5. (Color online) Temperature dependence of magnetization is plotted together with the inverse susceptibility.

maxima in both real and imaginary part of ac susceptibility. This temperature shifts somewhat to 90.5 K and the maximum broadens by the fast cooling synthesis indicating that fast cooling does not affect the temperature of magnetic phase transition very much. The temperature dependence of magnetization shows step increase of magnetization below 100 K which we associate with magnetic phase transition (Fig. 5). The temperature dependence of inverse susceptibility can be fitted above 180 K to a Curie–Weiss (CW) law giving the effective moment $\mu_{eff} = 2.82\ \mu_B$ and $\theta_p = 14.3$ K for the splat (Fig. 5). The positive value of θ_p indicates the ferromagnetic interaction in the sample. The effective moment is smaller than expected one for free uranium ion (3.6 μ_B), but higher than the moment of polycrystalline sample or single crystal. The value of θ_p is much smaller than in those cases [12,15,17].

Measurements of hysteresis loops indicate ferromagnetic behavior (Fig. 6). The magnetization does not saturate even at 18 T. Very large coercive field $\mu_0 H_c = 2.25$ T, which is comparable with measurements along magnetic hard axis on single crystal [17], is characteristic feature for the hysteresis loops of the $UNiSi_2$ splat (Fig. 6). Such enhancement of coercive field can be attributed to preferred orientation of crystallites along the hard magnetic axis or to pinning of domain walls on additional defects, which were introduced by rapid solidification, in the conditions of high anisotropy, producing very narrow domain walls. The coercive field is nearly the same for measurement with magnetic field applied along the splat and perpendicular to the surface of the splat which excluded preferential crystallization of crystals in the sample and large coercive force due to magneto-crystalline anisotropy. The huge coercive force can be in this manner attributed to pinning of narrow domain walls. Remnant magnetization and saturated magnetization both depend on applied magnetic field indicating shape anisotropy. The steps on the hysteresis loops for 2 K indicate magnetization processes in ferromagnetic material, which can be related to Barkhausen jumps. The hysteresis

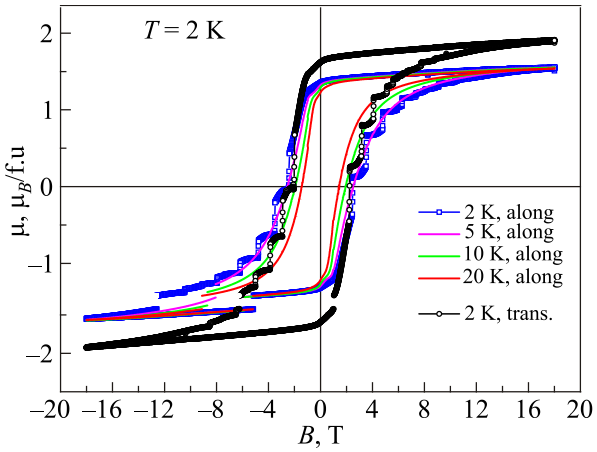

Fig. 6. (Color online) Hysteresis loops which were measured on a splat at various temperatures. Black pattern represents the measurement for transversal direction of magnetic field.

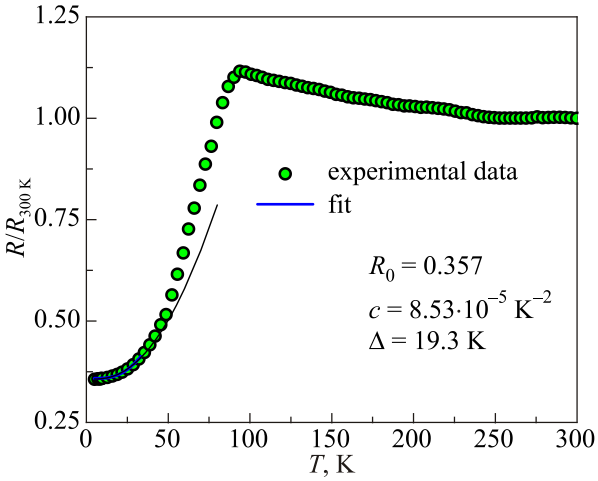

Fig. 8. (Color online) Temperature dependence of resistivity for the $UNiSi_2$ splat. The line represents the fit due to Eq. (1).

loop becomes smaller with increasing temperature; coercive force and remnant magnetization are reduced. Likewise Barkhausen jumps disappear with rising temperature. We wanted to study magnetic anisotropy in more details and that is why we compared measurements of hysteresis loop on the splat and powdered sample and the results are presented on Fig. 7. In the case of powdered sample the powder was fixed by glue to ensure that the magnetic field will not orient powder along easy magnetic axis. As can be seen (Fig. 7) the shape of hysteresis loops as well magnetic characteristics like coercive force and remnant magnetization are similar only the remnant and saturated magnetization at 18 T are higher for splat. The major difference is in Barkhausen jumps. In the case of splat there are several jumps on the loop in compare with only two main Barkhausen jumps on powdered splat.

The temperature dependence of the relative electrical resistivity, $R/R_{300}(T)$ is shown in Fig. 8. The resistivity

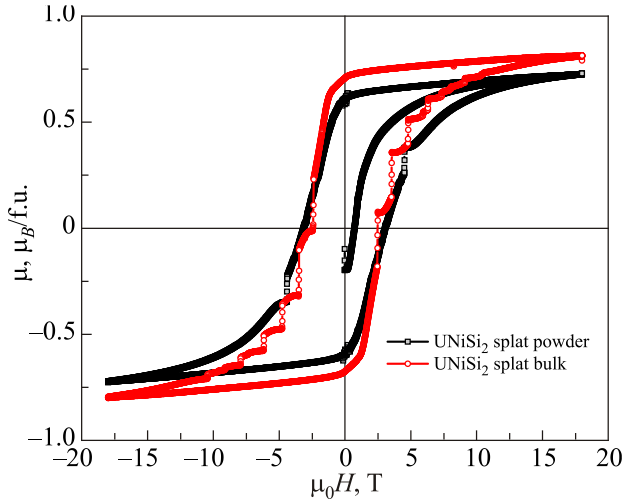

Fig. 7. (Color online) Hysteresis loops which were measured on a splat and on powdered splat.

curve resembles the resistivity curves of polycrystalline material [12,14]. The irregular shape of the sample did not allow the determination of absolute values of resistivity. The steep decrease of resistivity below 91 K we associate with transition to the magnetically ordered state. The low temperature part of the curve can be fitted by an expression, containing an exponential term, attributed to electron-magnon scattering:

$$\frac{R}{R_{300}} = R_0 + cT^2 \exp\left(-\frac{\Delta}{T}\right), \qquad (1)$$

where R_0 is dimension-less relative zero-temperature resistivity parameter and c has dimension [K^{-2}] used for fitting the relative resistivity data in temperature interval 2–33 K gives value $\Delta = 19.3$ K. This is somewhat smaller than the value determined on a polycrystalline material [13,15]. Weakly decreasing resistivity at high temperatures, also observed in [13], is generic for a broad class of U compounds with sizeable magnetic moments. They lead to a large spin-disorder resistivity, amounting to weak localization phenomena [18].

4. Conclusions

$UNiSi_2$ material has been for first time synthetized by the high vacuum splat cooling technique. The prepared splat beside the parent compound $UNiSi_2$ contains small amount of spurious phase as it was detected by XRPD, SEM and TEM techniques. The TEM revealed that majority of material consists of mixed structure formed by cylindrical or spherical nanocrystalline particles which are embedded into amorphous or nanocrystalline matrix with very fine nanoparticles. The remaining part of splat contains large crystalline blocks with the partially distorted crystal structure. Rapid solidification of the $UNiSi_2$ splats did not affect the magnetic transition but resulted in very high coercive force. Such enhancement of coercive force can be attributed to

pinning of domain walls on additional defects, which were introduced by rapid solidification, in the conditions of high anisotropy, producing very narrow domain walls. The steps on the hysteresis loops for 2 K indicate magnetization processes in ferromagnetic material, which can be related to Barkhausen jumps. Temperature of magnetic transition determined value of Δ resembles magnetic and electrical properties of from magnetization and resistivity measurements and the polycrystalline $UNiSi_2$ sample.

Acknowledgement

This work was supported by projects ERDF EU, No. ITMS26220120005 and VEGA 2/0010/16.

1. A.S. Edelstein, *J. Magn. Magn. Mater.* **256**, 430 (2003).
2. Y. Aoki, Y. Kobayashi, H. Sato, H. Sugawara, V. Sechovský, L. Havela, K. Prokeš, M. Mihalik, and A.A. Menovsky, *J. Phys. Soc. Jpn*. **65**, 3312 (1996).
3. M. Sigrist and Kazuo Ueda, *Rev. Mod. Phys*. **63**, 239 (1991).
4. S. Süllow, B. Becker, A. de Visser, M. Mihalik, G.J. Nieuwenhuys, A.A. Menovsky, and J.A. Mydosh *J. Phys.: Condens. Matter* **9**, 913 (1997).
5. H. Amitsuka, K. Kuwahara, M. Yokoyama, K. Tenya, T. Sakakibara, M. Mihalik, and A.A. Menovský, *Physica B* **281–282**, 326 (2000).
6. P. Samuely, P. Szabó, K. Flachbart, M. Mihalik, and A.A. Menovsky, *Physica B* **206–207**, 612 (1995).
7. M. Mihalik, A. de Visser, K. Bakker, L.T. Tai, A.A. Menovsky, R.W.A. Hendrikx, T.J. Gortenmulder, S. Maťaš, and N. Sato, *Physica B* **186–188**, 507 (1993).
8. V.P. Sinha, P.V. Henge, G.J. Prasad, G.K. Dey, and H.S. Kamath, *J. Alloys Comp.* **506**, 253 (2010).
9. M. Mihalik, P.F. Rogl, and A.A. Menovsky, *Physica B* **259–261**, 258 (1999).
10. A.G. Gukasov, P Rogl, P.J. Brown, M. Mihalik, and A. Menovsky, *J. Phys.: Condens. Matter* **14**, 8841 (2002).
11. Nhu-T.H. Kim-Ngan, I. Tkach, S. Mašková, L. Havela, A. Warren, and T. Scott, *Adv. Nat. Sci.: Nanosci. Nanotechnol.* **4**, 035006 (2013).
12. M. Ohashi, G. Oomi, K. Ishida, and I. Satoh, *J. Phys. Soc. Jpn.* **75**, 124 (2006).
13. V.A. Sidorov, P.H. Tobash, C. Wang, B.L. Scott, T. Park, E.D. Bauer, F. Ronning, J.D. Thompson, and Z. Fisk, *J. Phys.: Confer. Ser.* **273**, 012014 (2011).
14. E.I. Gladyshevsky, O.I. Bodak, and V.K. Pecharsky, in: *Handbook on the Physics and Chemistry of Rare Earth*, K.A. Gshneidner, Jr., and L. Eyring (eds.), North-Holland, Amsterdam (1990), Vol. 13, Chap. 88, p. 1.
15. D. Kaczorowski, *Solid State Commun.* **99**, 949 (1996).
16. T. Taniguchi, H. Morimoto, Y. Miyako, and S. Ramakrishnan, *J. Magn. Magn. Mater.* **177–181**, 55 (1998).
17. A. Das. S.K. Paranjpe, P. Raj, A. Satyamoorthy, K. Shashikala, and S.K. Malik, *Solid State Commun.* **114**, 87 (2000).
18. A.V. Kolomiets, J.-C. Griveau, J. Prchal, A.V. Andreev, and L. Havela, *Phys. Rev. B* **91**, 064405 (2015).